

Cite this: *Soft Matter*, 2012, **8**, 2671

www.rsc.org/softmatter

PAPER

Unexpected liquid crystalline behaviour of three-ring bent-core mesogens: bis(4-subst.-phenyl) 2-methyl-iso-phthalates†‡

Wolfgang Weissflog,^{*a} Ute Baumeister,^a Maria-Gabriela Tamba,^{‡a} Gerhard Pelzl,^a Horst Kresse,^a Rudolf Friedemann,^a Günther Hempel,^b Ricardo Kurz,^b Matthias Roos,^b Kurt Merzweiler,^c Antal Jáklí,^d Cuiyu Zhang,^d Nicholas Diorio,^d Ralf Stannarius,^e Alexey Eremin^e and Ulrike Kornek^e

Received 30th October 2011, Accepted 2nd December 2011

DOI: 10.1039/c2sm07064b

Three-ring bent-core bis(4-subst.-phenyl) 2-methyl-iso-phthalates exhibiting nematic, SmA and SmC phases are reported. The occurring mesophases have been identified by their optical textures and X-ray diffraction measurements which give also geometrical structural parameters like layer spacing and molecular tilt. Quantum chemical calculations on single molecules and X-ray structure analysis in the crystalline state indicate wide opening angles (about 155°) of the molecular legs due to the lateral methyl group in position 2 of the central phenyl ring. However solid state NMR spectroscopy in the liquid crystalline phases finds stronger molecular bending (bending angle to be about 138° in the SmA and about 146° in the nematic phase). Dielectric and SHG measurements give evidence that in the SmA phase a polar structure can be induced by application of an electric field which disappears in the isotropic liquid phase. The electric field not only leads to a slight textural change even in the SmA phase but also polar-type electric current response (P_S about 200 nC cm⁻²) is observed. This unusual electro-optical behaviour is discussed on the basis of the orientation of polar clusters formed by the bent molecules. In the paper we not only attempt to characterize the mesophases and to describe their physical properties, but we also show that these types of molecules represent the borderline between bent-shaped and calamitic liquid crystals.

1. Introduction

In 1923 Daniel Vorländer, the pioneer of liquid crystal chemistry, asserted that a bend in the molecular long axis of rod-like molecules reduces or prevents liquid crystalline behaviour. He found, for example, that the clearing temperatures directly correlate to the bond angle caused by oxygen, sulfur and nitrogen atoms in the centre of the molecules. From this point of view, mercury(II) should have a valence angle near to 180° in liquid crystalline diphenyl mercury derivatives.¹ On the other hand, since 1996 banana-shaped mesogens are a topic in the field of

liquid crystals, see reviews.²⁻⁴ Nearly all bent-core mesogens exhibiting banana phases consist of five or more aromatic rings. The question is what happens if the number of rings in bent-core molecules is reduced to four or three. In most cases, bent-core molecules consisting of four rings are not able to form liquid crystalline phases. But there are exceptions. In 2009, Weissflog *et al.* reported the unusual mesophase behaviour of substituted *N*-benzoylpiperazines which contain three phenyl rings together with a piperazine moiety.⁵ More recently, chiral ordered B₁ and B₇ phases, which are typical for banana-shaped liquid crystals, have been observed on four-ring asymmetric salicylideneimine derivatives.⁶ In contrast, the formation of nematic and smectic phases by 4-*n*-alkyloxybenzoic acid 4-[(3-benzylideneamino)phenylazo]phenylester should be re-examined because the phase type and transition behaviour reported are nearly identical with those of the alkyloxybenzoic acid used as starting materials.⁷

Bent three-ring mesogens can be subdivided into two types depending on the position of the bend in the molecules. If the bend of the molecular long axis results from a meta-substitution at one of the outer phenyl rings, one speaks about hockey stick-shaped mesogens. Remarkably, a SmC_{antclinic}–SmC_{synclinic} transition was observed for non-chiral hockey stick-shaped liquid crystals.⁸⁻¹⁰

In the other type of three-ring bent-core compounds a bent molecular fragment occurs in the centre of the molecules.

^aMartin Luther University Halle-Wittenberg, Institute of Chemistry, Physical Chemistry, von-Danckelmann-Platz 4, 06120 Halle, Germany

^bMartin Luther University Halle-Wittenberg, Institute of Physics, Betty-Heimann-Str. 7, 06120 Halle, Germany

^cMartin Luther University Halle-Wittenberg, Institute of Chemie, Inorganic Chemistry, Kurt-Mothes-Strasse 2, 06120 Halle, Germany

^dKent State University, Liquid Crystal Institute, Kent, Ohio, 44242, USA

^eOtto-von-Guericke University Magdeburg, Institute of Experimental Physics, Universitätsplatz 2, 39106 Magdeburg, Germany

† Electronic supplementary information (ESI) available. CCDC reference number 845881. For ESI and crystallographic data in CIF or other electronic format see DOI: 10.1039/c2sm07064b

‡ Present address: University of Hull, Department of Chemistry, Hull, HU6 7RX, UK.

Usually, three-ring molecules with a 1,3-phenylene unit are not able to form mesophases. This statement is only true, however, if the interaction forces are dominated by the molecular shape. If hydrogen bonds or microsegregation effects dominate, the molecular shape and the mesophase behaviour are not so clearly related. For example, bent phasmidic molecules bearing three alkoxy chains at both terminal phenyl rings (see Scheme 1a) often form columnar phases, as observed for correspondingly substituted benzoic anhydrides, gallic esters of 4,5-dinitrobenzoate, 3,5-diphenyl-1,2,4-triazoles, 3,5-distyrylpyridines, and furthermore.^{11–16} The molecular organisation can be modified by hydrogen bonding, as found for example for related urea derivatives and amido group containing mesogens.^{17,18} Furthermore, the strong tendency towards microsegregation is well-known for molecules bearing perfluoroalkyl chains. Hence, the compounds sketched in Scheme 1b exhibit smectic phases up to high temperatures.¹⁹ In contrast, liquid crystalline behaviour could not be observed for three-ring bent-core molecules bearing dimethylsiloxane units in the terminal chains (Scheme 1c), although these groups exhibit a very high tendency towards microsegregation, too.²⁰

If we exclude the dominating influence of microsegregation—so far that is possible—we should mention the liquid crystalline behaviour of three-ring bent-core compounds which contain five-membered heterocycles, for example, 1,3,4-thiadiazoles sketched in Scheme 1d and also 1,3,4-oxadiazoles, 1,2,4-oxadiazoles, 1,3-thiazoles, and 1,2,3-triazoles.^{21–26}

A comparison of such compounds containing different five-membered heterocycles shows that their bending angle (defined as the angle between the bonds of the central heterocyclic ring to the two outer phenyl rings) varies between about 135 and 160° depending on the number, type, and position of the heteroatoms. That means these molecules mostly forming calamitic mesophases are clearly more elongated in comparison to the 1,3-phenylene derivatives which should have a bending angle of 120° caused by the *meta*-substitution.

Up to now there are no liquid crystalline three-ring bent-core compounds which correspond to the simple formula shown in Scheme 1e–g independent of the chemical structure of the connecting groups X and Y between the three phenyl rings. For example, corresponding stilbene derivatives (Scheme 1e) exhibit crystalline modifications, only.²⁷ Pisipati *et al.*^{28,29} reported banana phases for two 1,3-phenylene bis(4-*n*-alkoxybenzoates),

Scheme 1f. However the results discussed in either papers have to be revised because these compounds definitely do not form a mesophase (see also Table 1).

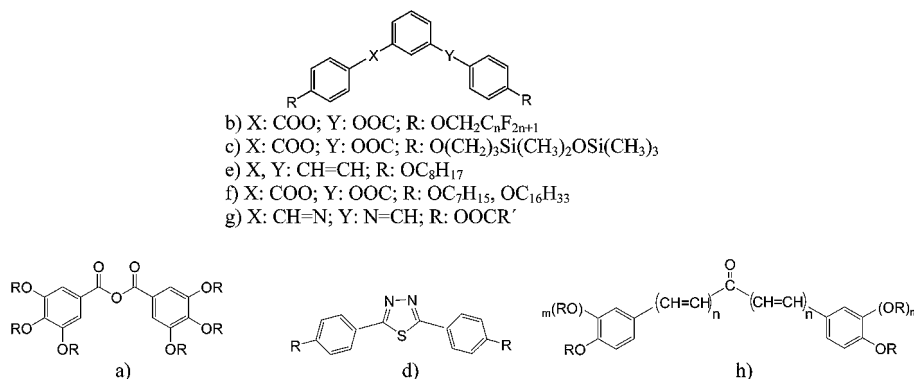
In 2010, Yuan Ming Huang and Qing-Lan Ma reported mesophases up to high temperatures on a new series of three-benzene-ring containing banana-shaped liquid crystals derived from 1,3-phenylenediamine, see Scheme 1g. Reproduction of two of the members using another reaction pathway proved that the materials under discussion exhibit melting points very different from the temperatures listed by Yuan Ming Huang *et al.*, and that the compounds do not form liquid crystalline phases.^{30,31}

Recently, K. A. Hope-Ross *et al.* reported a new family of bent C₂-symmetric liquid crystals.³² The molecules contain two phenyl rings only and the bend results from a carbonyl group, see Scheme 1h. Without additional C=C fragments the compounds are not liquid crystalline as expected (*n*: 0). Insertion of two C=C fragments results in nematic phases at low temperatures if the phenyl rings are 3,4-dialkoxy substituted (*n*: 1, *m*: 1). Extension of the unsaturated molecular range by insertion of four C=C fragments (*n*: 2, *m*: 0) yields nematic phases already for the 4-alkoxy substituted compounds. The supporting effect of

Table 1 Melting behaviour of isomeric three-ring bent-core compounds with and without a lateral methyl group in position Z (transition enthalpies in square brackets)

No.	Z	X	Y	Melting behaviour ^b
1a	H	COO	OOC	Mp. 71.4 [70.4]; T_{cryst} 50 °C
1b	H	OOC	COO	Mp. 125.2 [118.7]; T_{cryst} 100 °C
1c	H	COO	COO	Mp. 80.7 [85.7]; T_{cryst} 49 °C
2a	CH ₃	COO	OOC	Mp. 74.1 [43.7]; T_{cryst} 48 °C
2b	CH ₃	OOC	COO	Cr 98.2 [112.1] (SmC 86) ^a I
2c	CH ₃	COO	COO	Mp. 71.8 [65.4]; T_{cryst} 46 °C

^a Found by polarizing optical microscopy, could not be measured by DSC due to recrystallization. ^b The recrystallization temperature T_{cryst} was found by slow supercooling of the isotropic melt using the polarizing microscope.



Scheme 1 Different types of bent-core molecules containing two or three phenyl rings.

C=C fragments is well-known for a long time, for example, the nematic phases of 6-*n*-alkylhexadien-(2,4)-carboxylic acids can be explained this way.³³ Referring to the current paper the question arises, what is the real bending angle caused by a carbonyl group in such flexible molecules.

This paper describes the influence of a lateral methyl group attached to position 2 of the central phenyl ring, that is at the obtuse angle, of three-ring bent-core molecules on the meso-phase behaviour, see Scheme 2. To understand the unexpected liquid crystalline properties of 2-methylisophthalic acid diphenyl esters, different physical methods are employed: optical polarizing microscopy, DSC, dielectric, electro-optical and SHG measurements, X-ray diffraction measurements in the liquid crystalline and the crystalline solid state, and NMR studies in the liquid crystalline phases together with quantum chemical calculations.

2. Synthesis of new materials and methods of their physical investigation

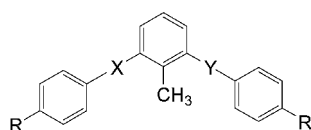
All the symmetrically and non-symmetrically constructed compounds **1–6** contain ester groups. The synthesis was carried out by reaction of substituted phenols and aliphatic hydroxyl compounds, respectively, with corresponding acids using standard procedures. In some cases the employment of protecting groups was helpful (Schemes S1–S3 in the ESI†). The experimental procedure and analytical data of representative examples are reported in the ESI†.

The phase transition temperatures and transition enthalpies were determined using a *differential scanning calorimeter* DSC Pyris 1 (Perkin Elmer).

The optical textures and field-induced texture changes were examined using a *polarizing microscope* DMRXP (Leica) equipped with a hot stage HT80 and an automatic temperature controller (Mettler Toledo).

To study the *electro-optical behaviour* the liquid-crystalline material was loaded into commercial cells of thickness 6 and 10 μm (EHC Corp. Tokyo). The cells were mounted in the heating stage of a polarizing microscope and a function synthesizer (Keithley 3910). The square-wave voltage and the triangular-wave voltage methods were employed for the experiments to determine the switching polarization.

Second harmonic generation (SHG) measurements have been performed in transmission geometry using a Nd:YAG laser (wavelength $\lambda = 1064$ nm, pulse duration 10 ns, repetition rate 10 Hz). The fundamental light beam was incident at an angle of 40° to the normal of the cell. The SHG signal was detected in transmission direction by a photomultiplier tube (Hamamatsu).



X - Y: COO - OOC; COO - COO; OOC - COO

Scheme 2 General formula of laterally methyl-substituted three-ring bent-core mesogens.

X-Ray investigations were carried out using Ni-filtered CuK α radiation and an area detector (HI-STAR, Siemens/Bruker). Surface alignment was obtained by slowly cooling a drop of the substance from the isotropic liquid on a glass plate on a temperature controlled heating stage. Samples in capillaries were aligned by a magnetic field in a temperature controlled oven.

Dielectric measurements were done with a Solartron Schlumberger Impedance Analyzer SI 1260 in combination with a Chelsea interface. The measurements were performed during cooling in the frequency range from 1 Hz to 10 MHz. A brass cell coated with gold was used as a capacitor. The distance between the electrodes was 60 μm.

The *NMR measurements* were performed on a BRUKER AVANCE II at resonance frequencies of 400 MHz (¹H) and 100 MHz (¹³C), respectively.

The *X-ray single crystal* data were collected on a Stoe IPDS I imaging plate diffractometer at 220 K with MoK α radiation. Lattice parameters: $a = 743.60(5)$, $b = 2706.4(2)$, $c = 1092.70(8)$ pm, $V = 2199.0(3) \times 10^6$ pm³, orthorhombic, space group *Pnma*, $Z = 4$, 10 751 reflections (2177 unique), $R(\text{int}) = 0.067$, 188 parameters, final R -values: $R_1(I > 2\sigma(I)) = 0.0394$, $wR_2(\text{all data}) = 0.0988$.

3. Results

3.1. Influence of the ester orientation in isomeric three-ring bent-core mesogens without and with a lateral methyl group

Usually, the direction of ester connecting groups strongly influences the type of mesophases and their thermal stability. Furthermore, the packing of the molecules within layer structures is changed because the dipole moments of two carboxylic groups can be added or compensated in the molecule. That can be interesting, for example, in search for SmC materials. There are numerous papers concerned with this problem for calamitic mesogens, see *e.g.* ref. 34–37. Six years ago, the mesophase behaviour of two complete series of each ten isomeric five-ring bent-core mesogens has been reported. In spite of their minor structural differences a variety of mesophases occur (SmCP_A, Col_{rec}, Col_{obl}) and the clearing temperatures vary from about 120 to 190 °C.³⁸ Recently, the strong influence of the direction of the carboxylic connecting groups on the mesophase behaviour of silylated bent-core molecules was found by Reddy *et al.*³⁹

Two series of each three isomeric compounds only differing in the direction of the ester connecting groups are shown in Table 1. Liquid crystalline phases could not be observed for the three-ring bent-core compounds **1a–c**, although the isotropic melts can be supercooled by about 20–30 K. The situation is changed if a methyl group is laterally attached to the obtuse angle of the molecule that is in position *Z*, see compounds **2a–c** in Table 1. Surprisingly, a smectic C phase could be proved for compound **2b**, that is bis(4-*n*-tetradecyloxyphenyl) 2-methylisophthalate. The mesophase exists in the metastable state only, nevertheless, this result has been the starting point to investigate further esters of 2-methylisophthalic acid in more detail. From the synthetic point of view the variation of the type and length of the terminal groups has been the possibility with the best prospect of success.

3.2 The mesophase behaviour of bis(4-subst.-phenyl) 2-methylisophthalates

Starting with the alkyloxyphenyl esters, an almost complete homologous series **3a–n** was prepared. The transition temperatures and enthalpies are listed in Table 2.

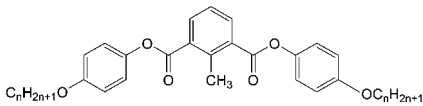
Surprisingly, liquid crystalline behaviour could be observed for all homologues of series **3**. A nematic phase is formed by the first ten homologues **3a–j**. The nonyloxy- and decyloxy-substituted compounds **3i** and **3j** exhibit a nematic–SmC dimorphism. The longer chain homologues **3k–n** have a smectic C phase only. All phases are metastable and most of them have only been observed by polarising microscopy. The nematic–isotropic transition temperatures show an alternation effect in dependence on the chain length, well-known for calamitic mesogens. The SmC transition temperatures increase with growing hydrocarbon chains up to the tetradecyloxy derivative **3l**, see Fig. 1.

The mesophase behaviour changes if the alkyloxy wing-groups are replaced by aliphatic acyl chains, see Table 3. The melting points are very high for the first members of the series, decrease however with lengthening the chains up to 91 °C (**4i**). In contrast to the alkyloxy compounds **3**, the thermal stability of the mesophases is higher by about 30 K. Both effects together result in enantiotropic SmA phases observed for the nonanoyl- and decanoyl-substituted homologues **4h** and **4i**, which are good candidates for further physical investigations.

To check the influence of the chemical structure of the wing-groups on the liquid crystalline behaviour of bis(4-subst.-phenyl) 2-methylisophthalates, further aliphatic groups are attached to both terminal positions. These compounds are listed in Table 4.

The alkyphenyl esters **5a–c** exhibit a nematic phase. The combination of these and/or further homologues could result in

Table 2 Transition temperatures (°C, for monotropic transitions in parentheses) and transition enthalpies [kJ mole⁻¹] of the bis(4-*n*-alkyloxyphenyl) 2-methylisophthalates **3a–3n**



No.	<i>n</i>	Cr	SmC	N	Is
3a	1	134.1, [38.3]	—	(85) ^a	·
3b	2	119.9, [38.5]	—	(103) ^a	·
3c	3	132.1, [45.4]	—	(68) ^a	·
3d	4	99.7, [44.0]	—	(83) ^a	·
3e	5	81.6, [54.2]	—	(67) ^a	·
3f	6	79.8, [58.9]	—	(70.5), [0.52]	·
3g	7	83.1, [49.4]	—	(66.0), [0.53]	·
3h	8	73.7, [55.3]	—	(71.9), [0.68]	·
3i	9	81.3, [72.8]	(54) ^a	(69.2), [0.93]	·
3j	10	82.9, [74.8]	(66) ^a	(72.7), [0.94]	·
3k	12	93.0, [97.4]	(78) ^a	—	·
3l^b	14	98.2, [112.1]	(86) ^a	—	·
3m	16	102.9, [128.2]	(83) ^a	—	·
3n	18	106.9, [140.8]	(79) ^a	—	·

^a Found by polarizing optical microscopy, could not be measured by DSC due to recrystallization. ^b Compound **3l** corresponds to **2b** in Table 1.

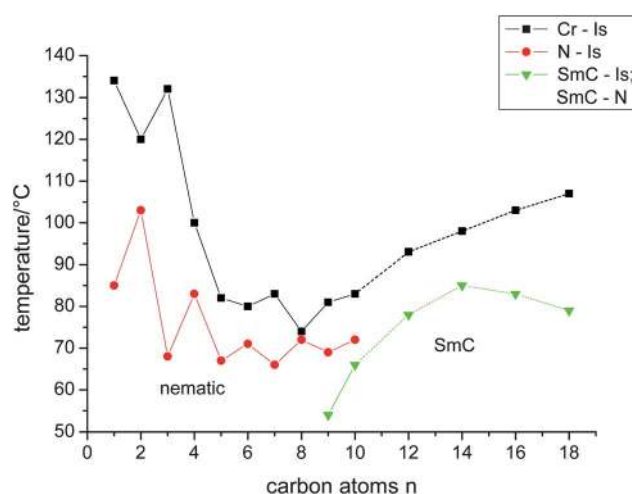
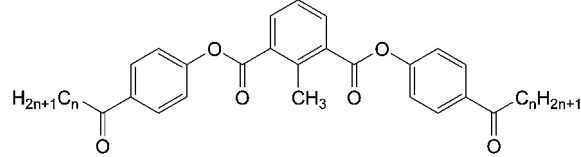


Fig. 1 Course of the mesophase transition temperatures on cooling in the homologous series **3a–3n**.

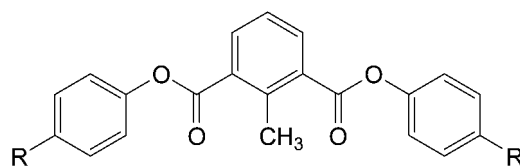
a nematic mixture stable near to room temperature, which could serve as materials using the flexoelectric effect. In contrast, the β -substitution of the 4-ethylphenyl esters by a cyano or aceto group gives the non-mesomorphic compounds **5d** and **5e**. A metastable SmA phase could be observed for compound **5f** with a number of single CH₂ units amounting to 16 per chain. The ω -substitution of a pentadecyloxy wing-group with the methoxycarbonyl moiety (compound **5g**) results in the loss of liquid crystalline properties in comparison to the alkyloxy substituted compounds **3l** and **3m**. If the hydrocarbon chains are connected to the outer phenyl rings by ester groups, these can have different directions. In the case of alkyl benzoate moieties, see compounds **5h** and **5i**, mesophases could not be observed although the melting points are relatively low. Inversion of the outer ester groups gives compounds **5j–l**, which are liquid

Table 3 Transition temperatures (°C, for monotropic transitions in parentheses) and transition enthalpies [kJ mole⁻¹] of the bis(4-*n*-alkanoylphenyl) 2-methylisophthalates **4a–4i**



No.	<i>n</i>	Cr	SmA	N	Is
4a	1	202.6, [53.3]	—	(92) ^a	·
4b	2	229.7, [62.3]	—	—	·
4c	3	175.5, [50.5]	—	(82) ^a	·
4d	4	187.7, [77.4]	—	(96) ^a	·
4e	5	159.8, [59.2]	—	(90) ^a	·
4f	6	166.0, [76.9]	—	(99) ^a	·
4g	7	129.8, [58.1]	(107) ^a	—	·
4h	8	101.7, [56.3]	114.7, [8.1]	—	·
4i	9	90.8, [45.2]	118.6, [9.6]	—	·

^a Found by polarizing optical microscopy, could not be measured by DSC due to recrystallization.

Table 4 Transition temperatures (°C, for monotropic transitions in parentheses) and transition enthalpies [kJ mole⁻¹] of the bis(4-*n*-subst.-phenyl) 2-methylisophthalates **5a–5l**

No.	R	Cr	SmC	SmA	N	Is
5a	C ₈ H ₁₇	48.9, [30.0]	—	—	(39) ^a	·
5b	C ₉ H ₁₉	55.7, [32.7]	—	—	(46) ^a	·
5c	C ₁₂ H ₂₅	56.8, [43.8]	—	—	(50.3), [5.4]	·
5d	CH ₂ CH ₂ CN	125.7, [41.8]	—	—	—	·
5e	CH ₂ CH ₂ COCH ₃	155.0, [62.3]	—	—	—	·
5f	CH ₂ CH ₂ OCC ₁₂ H ₂₅	83.0, [76.9]	—	(59) ^a	—	·
5g	OC ₁₅ H ₃₀ COOCH ₃	104.4, [146.4]	—	—	—	·
5h	COOC ₆ H ₁₃	69.7, [42.9]	—	—	—	·
5i	COOC ₁₂ H ₂₅	73.1, [86.3]	—	—	—	·
5j	OOC ₇ H ₁₅	83.1, [36.0]	—	—	100.1, [0.65]	·
5k	OOC ₁₅ H ₃₁	92.1, [64.5]	109.8, [10.3]	—	—	·
5l	OOC ₁₅ H ₃₀ Br	88.2, [91.5]	(78) ^a	(82.5) ^a	—	·

^a Found by polarizing optical microscopy, could not be measured by DSC due to recrystallization.

crystalline materials. The ester of the octanoic acid **5j** exhibits an enantiotropic nematic phase sufficiently broad for physical measurements. The palmitic acid derivative **5k** has a SmC phase from 92–110 °C. The ω-substitution of the same compound with bromo atoms reduces the clearing temperature by 17 K, nevertheless, a SmA–SmC dimorphism could be proved for compound **5l**.

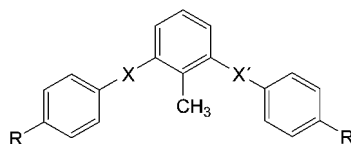
To study the effect of stiffness of the whole molecules, the connecting groups X and X' were changed to be more flexible. The insertion of methylene, ethyleneoxy, or propyleneoxy fragments between the outer phenyl rings and the 2-methylisophthalic ester moiety could make the molecules more rod-like. But compounds **6a–c** do not form mesophases in spite of their low melting points, see Table 5.

Summarizing this part, we state that three-ring bent-core compounds derived from 2-methylisophthalic acid can form mesophases. Optical studies give hints for nematic, SmA and SmC phases, respectively. In the following section physical

measurements are reported which should prove the type of mesophases, their structures and physical properties. Furthermore we want to find out why especially these esters are able to form mesophases.

3.3 X-Ray crystal structure analysis of compound **4b**

The liquid crystalline behaviour of bis(4-subst.-phenyl) 2-methylisophthalates is unexpected and it is in contradiction to the experimental experiences summarized in Section 1. Looking at Table 1 again one can see that only the esters of 2-methylisophthalic acid are able to form mesophases. Furthermore, it seems that the mesophases observed are more typical for calamitic molecules. Therefore the question arises what is the real shape of the molecules. The bending angle of diphenyl isophthalates (*e.g.* no. **1b**) should be nearly 120°. Furthermore, it is known that resorcinol bisbenzoates (*e.g.* no. **1a**) exhibit a bending angle of about 120°. With respect to banana-shaped

Table 5 Melting behaviour of further esters of the 2-methylisophthalic acid having flexible connecting groups X in comparison to compound **3j**

No	R	X	X'	Cr	SmC	N	Is
3j	OC ₁₀ H ₂₁	OOC	COO	82.9, [74.8]	(66) ^a	(72.7), [0.94]	·
6a	OC ₁₀ H ₂₁	CH ₂ OOC	COOCH ₂	56.0, [82.6]	—	—	·
6b	COC ₉ H ₁₉	OCH ₂ CH ₂ OOC	COOCH ₂ CH ₂ O	70.6, [62.8]	—	—	·
6c	OC ₈ H ₁₇	OCH ₂ CH ₂ CH ₂ OOC	COOCH ₂ CH ₂ CH ₂ O	63.8, [73.3]	—	—	·

^a Found by polarizing optical microscopy, could not be measured by DSC due to recrystallization.

liquid crystals the conformations of five-ring compounds derived from 2-methylresorcinol dibenzoate have been investigated by ^1H and ^{13}C NMR methods. The bending angle was measured in the liquid crystalline phase to be near to $120^\circ \pm 5^\circ$.⁴⁰ Therefore, it can be assumed that compound **2a** has a similar molecular shape. However, there is no reference in the literature to the molecular conformation of diphenyl 2-methylisophthalates like compound **2b**.

We were able to grow single crystals of compound **4b** by crystallisation from a dimethylformamide/ethanol mixture. Compound **4b** crystallizes in orthorhombic space group *Pnma* with four formula units per unit cell. The crystal structure of **4b** consists of discrete molecules that exhibit no unusual short intermolecular contacts. C–C, C–H and C–O bond lengths are within the expected ranges (see Table S1†). The molecular structure of **4b** (Fig. 2a and b) exhibits a crystallographic mirror plane passing through the atoms H1, C1, and C4 of the central

aromatic ring and C5 and H4 of the methyl group attached to C4. The conformation of **4b** is characterized by a non-co-planar arrangement of the carboxylate group C6–O1–O2 with respect to the central aromatic ring and the terminal EtCOC₆H₄ unit (Fig. 2b). In the case of the central aromatic ring the CO₂-plane is rotated by -142° along C3–C6 and for the terminal EtCOC₆H₄ unit a torsion angle C6–O1–C7–C12 of 123° is observed. The latter value is expected for a phenyl benzoate moiety, whereas the former would be near 180° in a phenyl benzoate without a substituent in the 2-position.^{41–43} The comparatively strong deviation is clearly determined by the steric influence of the methyl group. Interestingly, this leads to a conformation with both CO groups pointing to the same side out of the plane of this ring as necessary for the mirror symmetry of the molecule (Fig. 2b and c). Another consequence is the unusually wide bending angle of the molecular core defined by the centres of the aromatic rings amounting to 156° (Fig. 2a).

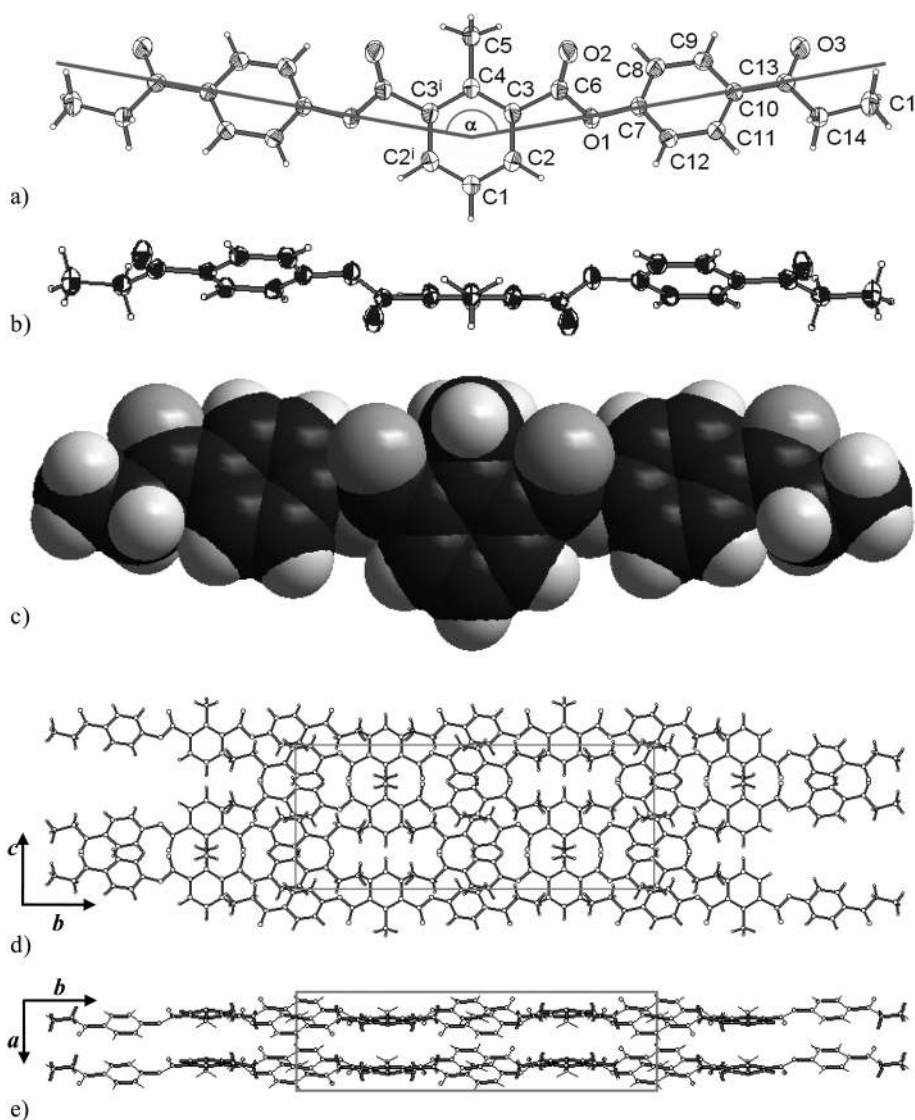


Fig. 2 Structure of **4b** in the crystal: (a) molecular structure with atom labelling showing the bending angle α of the core (thermal ellipsoids shown at the 50% level), (b) projection of the molecular structure along the direction C4–C1, (c) space filling model, (d) projection of the crystal packing along *a*, and (e) projection of the crystal packing along *c*.

The crystal packing (Fig. 2d and e) displays a strictly parallel arrangement of the long molecular axes with respect to the crystallographic b axis and hence to one another. Each of the two mirror planes of the unit cell at $y = 1/4b$ and $y = 3/4b$ bisects the molecules along the atoms C1, C4 and C5. The aromatic rings of the wing groups display a layer-like arrangement perpendicular to the crystallographic y axis at $y = 0$ and $y = 1/2$. Thus the typical “nematogenic” shift of the molecules along their long axes giving a partial core–tail packing is probably due to the dense packing of the outer phenyl rings and the comparatively stronger separation of the central rings forced by the sterical requirements of the methyl substituent.

The single crystal structure analysis of compound **4b** shows the basic difference between compounds **1a**, **1b**, **2a** and **2b**. The molecules of **1a**, **1b**, and **2a** exhibit a bending angle near to 120° (defined by the centres of the three aromatic rings) whereas the angle between the two legs of compound **4b** (corresponds to **2b**) is extended to 156° . It should be mentioned, however, that the molecular conformation measured in the crystalline state can be similar to that in the liquid crystalline state but it may as well strongly differ from it.

According to the crystal structure of **4b** the compounds under study consist of molecules which are only slightly bent, but clearly different from rod-like ones.

3.4 X-Ray investigations on the liquid crystalline phases

X-Ray diffraction measurements have been performed on powder-like and surface-aligned samples of compounds **4h**, **4i**, **5j** and **5k** to prove the type of mesophase and to determine geometric structure parameters like layer spacing and molecular tilt. The two-dimensional (2D) diffraction patterns for these compounds are presented in Fig. 3 and calculated data in Table 6.

The smectic phases of **4h** and **4i** display the typical X-ray patterns for a SmA phase, strong layer reflections with their second order on the meridian and a diffuse outer scattering with maxima on the equator of the pattern (Fig. 3a–d). The outer diffuse scattering with its maximum at $d = 0.46$ nm indicates a liquid-like disorder of the molecules within the layers with their long axes on average parallel to the layer normal. The layer spacing of 3.5 nm for **4h** is significantly shorter than the average molecular length of about 4.0 nm estimated by molecular modelling using the core structure found in the crystalline solid state of compound **4b** (see Fig. 4, the stronger bend of the core found by NMR measurements would reduce the average molecular length to about 3.7 to 3.8 nm). Such a short layer distance could be possibly explained by partial intercalation of antiparallel pairs of essentially linear molecules caused by the space-consuming CH_3 substituent in the 2-position of the central phenyl ring (see Fig. 4d). That means **4h** with its comparatively short terminal chains behaves like a modified calamitic molecule which is in accordance with the phase behaviour of the shorter chain derivatives forming monotropic nematic phases on very strong supercooling of the isotropic liquid, with the parallel packing of the overall-linear shaped molecules of **4b** in the crystal (see Section 3.3: X-ray crystal structure analysis of **4b**), and with the results of the NMR measurements concerning the orientation of the chains (see Section 3.7). The medium-sized chains may give

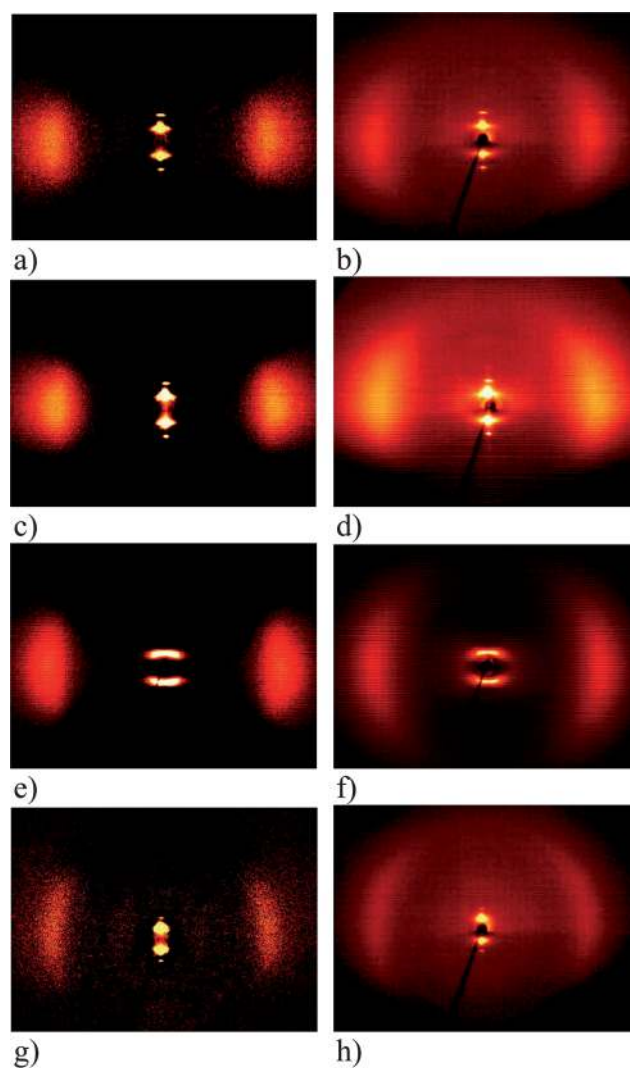


Fig. 3 X-Ray patterns for aligned samples of compounds **4h** (a and b: 110°C), **4i** (c and d: 115°C), **5j** (e and f: 80°C) and **5k** (g and h: 105°C) on cooling; (b, d, f, and h) original wide angle patterns and (a, c, e and g) the same patterns but the scattering of the isotropic phase has been subtracted to enhance the effect of the distribution of the outer diffuse scattering.

rise to stronger segregation effects changing the phase type from nematic to SmA. The polar cores of the molecules may even generate a packing with SmAP_A -like clusters as shown in Fig. 4e.

Another layer structure explaining the difference between the molecular length and the layer distance would be a SmAP_A like packing mode of on average overall bent-shaped molecules (Fig. 4f). Here, the bent aromatic core is unchanged, but the terminal chains are rotated around the aryl–COR bond. In this case the molecules would behave “banana”-like, which could also be initiated by the CH_3 substituent, the preferred orientation of the terminal chains resulting in an on average overall bend of the molecules compensating the more bulky central part of the molecules in the packing. This packing is more likely for a stronger bend of the core.

The X-ray patterns of the octanoic acid ester **5j** in the nematic phase aligned in a magnetic field exhibit strong dumbbell-like

Table 6 X-Ray data for compounds **4h**, **4i**, **5j** and **5k**: T —measuring temperature in °C, n —order of the layer reflection, 2θ —diffraction angle in °, and d — d value in Å

T	n	2θ	d	Layer distance
Compound 4h				
110	1	2.545	34.7	34.9
	2	5.035	17.5	
		19.1 ^a	4.6 ^a	
Compound 4i				
115	1	2.402	36.8	36.7
	2	4.819	18.3	
		19.2 ^a	4.6 ^a	
Compound 5j				
80		2.735 ^a	32.3 ^a	
		19.3 ^a	4.6 ^a	
Compound 5k				
105	1	2.020	43.7	44.2
	2	3.957	22.3	
		18.9 ^a	4.7 ^a	

^a Values for the maxima of the diffuse scattering.

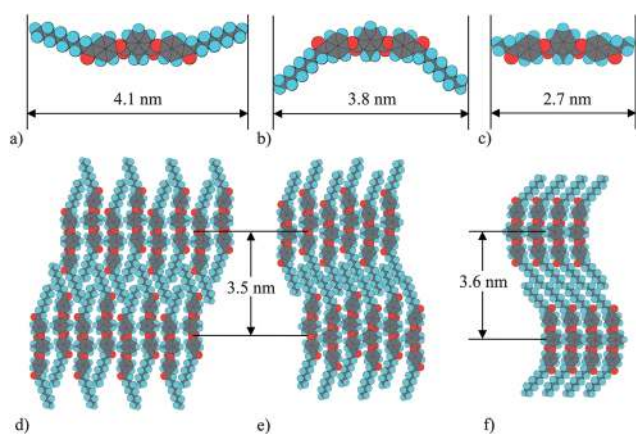


Fig. 4 Molecular models (Chem3D, Cambridge Soft.Com, 2000) for **4h** with two extreme chain orientations showing the molecular length. Model (a) has been constructed from the molecular structure of **4b** in the single crystal (c) by adding six CH₂ groups to each side chain in all-*trans* configuration, for model (b) the chains have been rotated by 180° about the C_{phenyl}–C_{C=O} bond; (d and e) possible schematic packing in the SmA phase for molecules with preferably overall stretched shape, (d) non-polar packing mode, (e and f) SmAP_A packing mode, and (f) for molecules with preferably bent shape.

scattering maxima in the small angle region indicating SmC type smectic clusters (Fig. 3e and f). Since the outer diffuse scattering shows only two maxima lying on the equator of the patterns, the molecular long axes are clearly aligned on average normal to the equator, *i.e.* parallel to the magnetic field, and hence the separation of the maxima of the inner scattering is a measure of the tilt of the molecules within the smectic-like layers of the clusters. This tilt is about 25°.

Compound **5k** with its much longer terminal chains shows layer reflections of the first and second order on the meridian of the 2D X-ray pattern and an outer diffuse scattering like **4h** and **4i**, but the azimuthal distribution of this scattering is much broader (see Fig. 3g and h), indicating a tilt of the long molecular axes with respect to the layer normal. Obviously, the average tilt

is not strong enough to cause a clear splitting of the halo into four maxima, but a fit of the experimental curve by four Gaussian curves yielded maxima at $\chi = 76, 102, 250,$ and 285° and from these values the tilt can be roughly estimated to $\tau = 15^\circ$ (see the χ -scan in Fig. S1†). Together with the layer spacing $d = 4.4$ nm an average effective molecular length of $L = d/\cos \tau = 4.6$ nm can be calculated. This value is also very short compared with the average molecular length of about 5.0 to 5.2 nm estimated by molecular modelling, and similar packing modes as discussed above for the SmA phase have to be considered but with an additional tilt of the long molecular axes with respect to the layer normal.

3.5 Electro-optical and SHG measurements

Electro-optical and SHG measurements were done on the SmA phases of compounds **4i** and **4h**. The electro-optical behaviour of these three-ring compounds is quite unusual. In electric fields the texture change was only minor after manifold switching processes, expressed in a slight smoothing of the pattern. The changes are independent of the polarity of the electric field as shown in Fig. 5a–c for DC experiments. The electro-optical behaviour using non-coated cells for AC fields is demonstrated in Fig. 5d–f. Because the field-induced texture is the same in the field-on and field-off states we can assume that the switching is based on the collective rotation of the molecules around their long axes. The observed texture change resembles the optical change in the SmAP_R phase, reported recently by Keith *et al.*⁴⁴

No field-induced tilt could be detected and the texture is not sensitive to the polarity of the electric field, as recently reported for a SmA phase formed by a four-ring bent-core compound.⁵

Current response measurements were done using triangular and square-wave voltages. Fig. 6 shows a pronounced current response, which often consists of two overlapped peaks. The peaks were hard to separate from each other. The spontaneous (or induced) polarization was estimated from the integral of the current transient peak.⁴⁵

To distinguish between the ionic contribution (extensive) from the polar and dielectric contributions (intensive), we performed the measurements of the induced polarization in cells of two different thicknesses of 6 and 10 μm (Fig. 7a). In the SmA phase, the polarisation is nearly the same in both cells, indicating that the polarization is mainly induced by alignment of the molecular dipoles, presumably, organized in clusters. In contrast, the switching polarization in the isotropic phase is proportional to the cell thickness and obviously results from the accumulation of ionic charges on the electrodes. This process is accompanied by a considerable increase of conductivity on the transition into the SmA phase (Fig. 7b). The reason why the ionic contribution is not evident in the SmA phase is probably due to longer relaxation times of the ionic contribution and the small electric conductivity of the mesophase.

The switching times at different temperatures are determined from the time dependence of the electric currents under rectangular electric waveforms shown below. Taking the switching time from the position of the current peak, we see that it is decreasing with increasing temperatures, even above the transition to the isotropic texture from about 0.5 ms at the SmA transition to 0.15 ms slightly above the SmA–isotropic transition, as seen in Fig. 8.

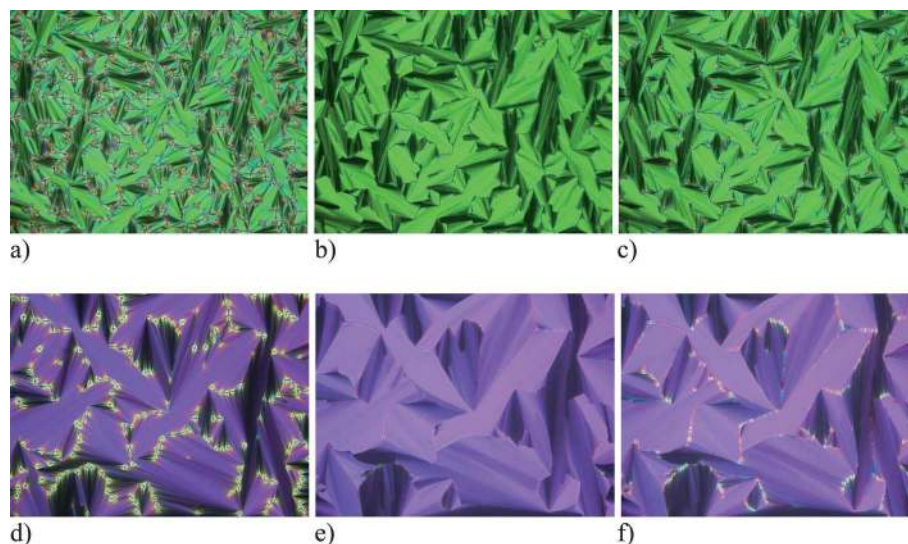


Fig. 5 Influence of electric fields on the SmA texture of compound **4i**. (a–c) DC field, 6 μm cell polyimide-coated E.H.C. cell, 110 $^{\circ}\text{C}$: (a) 0 V, (b) ± 100 V, and (c) after switching off the field; (d–f) AC field, 5 μm non-coated E.H.C. cell, 87 $^{\circ}\text{C}$: (a) 0 V, (b) 10 Hz, 314 V, and (c) after switching off the field.

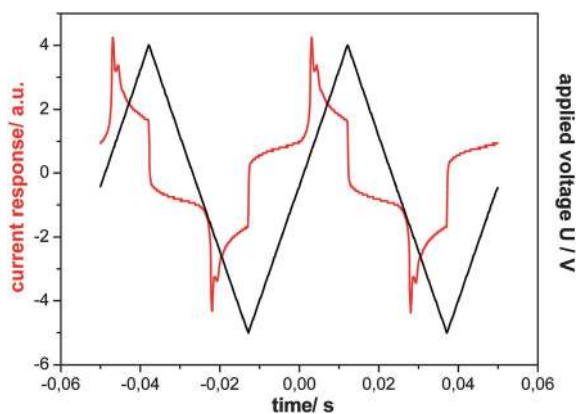


Fig. 6 Compound **4i**, current response on the SmA phase at 95 $^{\circ}\text{C}$ in dependence of time and voltage (6 μm polyimide-coated E.H.C. cell, AC field, 20 Hz), $P_S = 200 \text{ nC cm}^{-2}$.

The electro-optical behaviour of the homologous compound **4h** is nearly the same as reported above for compound **4i**. Additionally, measurements of the second harmonic were

performed. A remarkable SHG signal was detected in the SmA phase which disappeared upon the transition into the isotropic phase (Fig. 9). That means there is a polar order in the SmA phase which disappears in the isotropic liquid state. The field-dependence of the signal has a shape corresponding to a Langevin-type behaviour of the field-induced polarization.

The results of the electro-optical studies and SHG measurements are in good agreement. It seems obvious though that the SmA phase in compounds **4i** and **4h** is not ferroelectric in the field-free state. A strong electric response may be attributed to randomly oriented polar smectic clusters which also remain in the isotropic phase sufficiently close to the clearing point. The existence of clusters in the isotropic phase of bent-core mesogens has been proved by NMR spectroscopy.⁴⁶ Even in the smectic and isotropic phase, such clusters were recently found in binary mixtures of some bent-core and rod-shaped molecules.⁴⁷ The field-induced orientation of the clusters also accounts for the slow dynamics. The reduction of the switching time in Fig. 8 with increasing temperature can be attributed to a decrease of the cluster size and of the viscosity of the continuous medium. The increase of the current at increasing temperature under constant

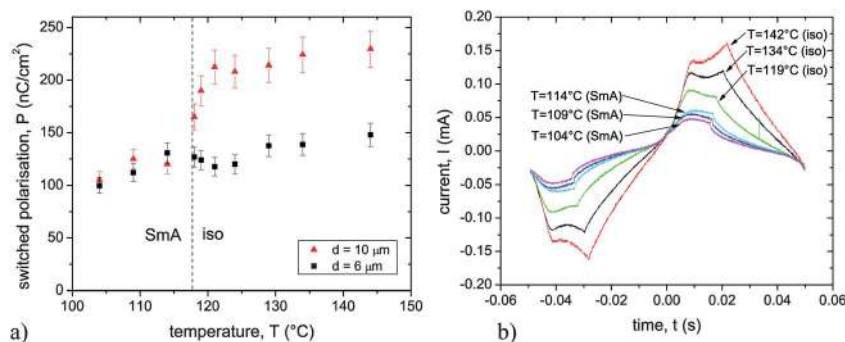


Fig. 7 Compound **4i**: (a) field-induced polarization in dependence on the temperature ($f = 10 \text{ Hz}$, $E_{pp} = 18 \text{ V } \mu\text{m}^{-1}$), the thickness dependent growth of P in the isotropic phase is attributed to the ionic polarization, and (b) selected current response curves in the SmA and the isotropic phase.

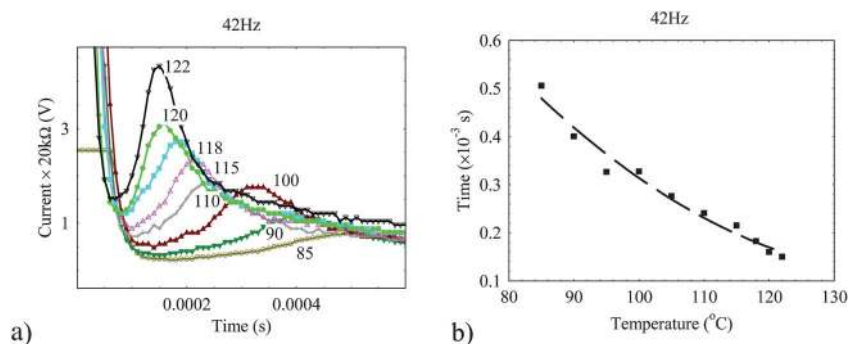


Fig. 8 Compound **4i**, measurement of the switching times, using an AC electric field, 42 Hz, $E = 20 \text{ V } \mu\text{m}^{-1}$. (a) Current–time behaviour at different temperatures; (b) decreasing switching times with increasing temperatures.

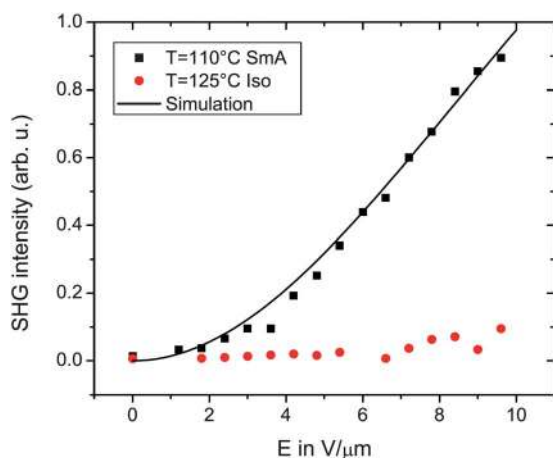


Fig. 9 Intensity of the SHG signal in compound **4h** as a function of the electric field in the SmA and isotropic phases. The simulation curve corresponds to a fit by the Langevin process.

electric fields is probably due to the increasing slope of the Langevin process at higher temperatures. We note that a similar electric current behaviour was also found in the nematic and isotropic phase of **5j**, where the smectic clusters were clearly seen in SAXS measurements.

3.6 Dielectric measurements

Three materials exhibiting SmA (**4i**), SmC (**5k**), and nematic phases (**5j**), respectively, have been studied by dielectric measurements.

The investigations on compound **4i** could only be performed on non-oriented samples. The dipole components in the direction of the molecular long axes compensate each other. Therefore, no relaxation related to the reorientation about the short axes is visible. The high dielectric permittivity in the SmA phase and the even stronger increase with decreasing temperature indicate an increasing positive correlation of the dipole moments perpendicular to the layer normal, see Fig. 10.

The relaxation frequency of about 3 MHz at 78 °C for the reorientation about the long axes of the molecules is much lower as observed for “classical” SmA phases formed by calamitic molecules. All of these can be interpreted as a tendency to form

polar phases or polar clusters at lower temperatures as already reported for five-ring bent-core materials.⁴⁸

The sample of compound **5k** was by chance oriented more in the planar way. No relaxation could be detected till 5 MHz. Also the relatively low dielectric permittivity in the SmC phase proves no ferroelectric short range structure, see Fig. 11.

Substance **5j** behaves from the dielectric point of view like a classical nematic one with negative dielectric anisotropy, see Fig. 12. No relaxation in the parallel direction (p) due to the symmetry of the molecule and no MHz relaxation in the perpendicular direction (s) are observed, because this relaxation appears at higher frequencies out of our experimental range.

3.7 Solid-state NMR investigations of the molecular conformations

NMR studies were performed in the nematic phase of compound **5j** and in the SmA phase of compound **4i**. The orientation of the director by the magnetic field was not only good in the nematic but surprisingly also in the smectic A phase. The samples were investigated with solid-state NMR methods. Here the orientation dependence of the dipolar coupling between neighbored ^1H nuclei as well as that between ^1H and ^{13}C was exploited. Previous works used the anisotropy of the ^{13}C chemical shift to get information about tilt angles of atomic groups with respect to the director.⁴⁹ This procedure, however, requires knowledge of the chemical shift tensor, *i.e.* of its main values as well as of its orientation in the molecular part.

Alternatively, utilization of dipolar interaction is advantageous in cases of poorly known chemical-shift tensors. The

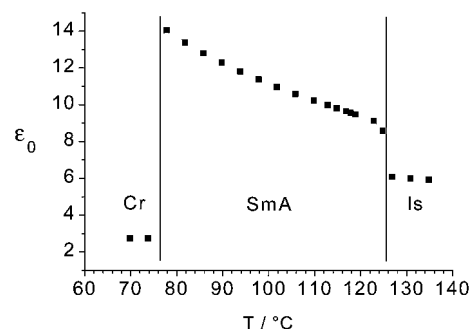


Fig. 10 Low frequency limit of the dielectric permittivity of substance **4i**.

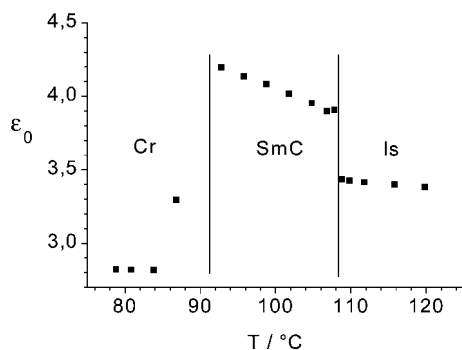


Fig. 11 Dielectric permittivities of substance **5k** versus temperature.

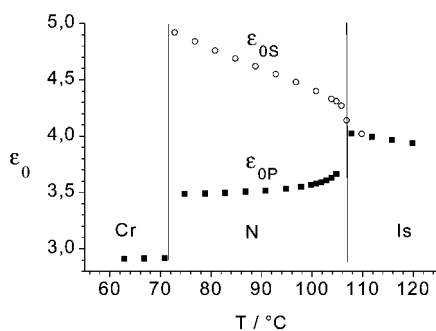


Fig. 12 Dielectric permittivities of substance **5j**. The sample was oriented by a magnetic field parallel (p) and perpendicular (s) to the nematic director.

dipolar tensor is oriented strictly along the connection line of the interaction nuclei, and its strength can be calculated easily, see below. In other cases also the dipolar interaction was used for the investigation of banana-shaped liquid crystals, see for example ref. 50.

Improved methods could yield experimental values with higher accuracy. The dipolar coupling between two nuclei with spin 1/2 (for example, ^1H and ^{13}C) depends on the molecular geometry. This can be expressed as a relation between the coupling constant ν , the magnitude r of the vector \mathbf{r} connecting the two nuclei, and the angle θ between \mathbf{r} and the external magnetic field \mathbf{B}_0 :

$$\nu = \nu_D S(3\cos^2 \theta - 1)$$

whereby the prefactor ν_D is equal to

$$\frac{3\mu_0\gamma^2\hbar}{16\pi^2} \times \frac{1}{r^3} (^1\text{H}-^1\text{H} \text{ coupling}) \text{ or } \frac{\mu_0\gamma_C\gamma_H\hbar}{8\pi^2} \times \frac{1}{r^3} (^{13}\text{C}-^1\text{H} \text{ coupling}).$$

(γ_H and γ_C are the gyromagnetic ratios of ^1H and ^{13}C , respectively, μ_0 is the permittivity of the vacuum, and $\hbar = h/2\pi$ is the reduced Planck's constant). S is the order parameter. Hence from the coupling constant of a spin pair we could calculate one of the quantities r , S , and θ relevant for this pair if the other parameters were known. If we align the directors along the field of the NMR magnet, θ also represents the angle between r and the average molecule axis. In our case we assumed usual values for atomic distances. S was estimated from coupling constants which belong

to spin pairs of the central ring; here r and θ are known. Now with known r and S values the coupling constants were direct measures of the tilts of certain C–H- and H–H-connection lines against the molecular axis. This way we obtained data about the tilt of whole atomic groups (rings, methylenes) against this axis which in a certain manner gives an estimate of the molecular bending angle.

The samples were aligned in the field of the NMR magnet (flux density: 9.4 T) by heating them to the isotropic phase and subsequently cooling slowly down to the mesophase. The orientation was checked by recording ^1H spectra (the dipolar splitting observed at this manner is not visible in the spectrum of a non-oriented sample). Furthermore, the line positions in the proton-decoupled ^{13}C spectra obtained in the experiments mentioned below are unambiguous indications of whether or not the samples were oriented.

The ^1H - ^{13}C couplings were investigated by a cross-polarization method. Here we observed the oscillatory polarization transfer between the systems of proton spins and ^{13}C spins. The frequencies of these oscillations give the coupling constants. To avoid that these values are influenced by proton–proton couplings the protons were irradiated under the Lee–Goldburg condition^{51,52} by which these unwanted couplings are suppressed. Typical interferograms representing the polarization-transfer oscillations are shown in Fig. 13.

Proton–proton couplings were estimated by a novel method.⁵³ It produces an initially strong spatial gradient in the proton polarization by burning holes in this magnetization distribution. If neighbored protons have different polarizations they start to exchange their oscillatory polarizations in a very similar manner as mentioned above for the proton–carbon polarization exchange. Again, the frequency of this oscillation represents the coupling constant. Typical interferograms and their spectra are shown in Fig. 14.

All NMR experiments were performed at resonance frequencies of 400 MHz (^1H) and 100 MHz (^{13}C). The radio-frequency field strengths correspond generally to nutation frequencies of 60 kHz at both channels with an exception during the Lee–Goldburg cross-polarization: here the ^{13}C nutation frequency was enhanced to 73.48 kHz together with a resonance offset of 42.43 kHz to match the conditions required for the polarization transfer. In the 2D experiments between 60 and 170 different signals were recorded; for each of them between 100 and 240 scans were accumulated. The NMR experiments were performed at temperatures of 9 K below the clearing point for **4i** and 7.5 K below the clearing point for **5j**.

As mentioned above from the dipolar couplings in the central ring the order parameters could be calculated to be 0.75 ± 0.01 (**4i**) and 0.61 ± 0.02 (**5j**). The difference is as expected because **4i** exhibits a SmA phase whereas **5j** exhibits the nematic one. The next step is the calculation of the tilt of the outer phenyl rings. Using the C–H couplings of the lateral (protonated) carbons of these rings (3.50 kHz for **4i**, 3.0 kHz for **5j**) the fast reorientation of these rings must be regarded. The H–H coupling (11 kHz for **4i**) is insensitive to this reorientation; the corresponding connection vector points along the ring rotation axis. From these values we obtained tilts of the outer phenyl rings with respect to the molecular long axis of 21° and 18° for **4i** and **5j**, respectively. Therefore the bending angles of the three-ring aromatic core turn

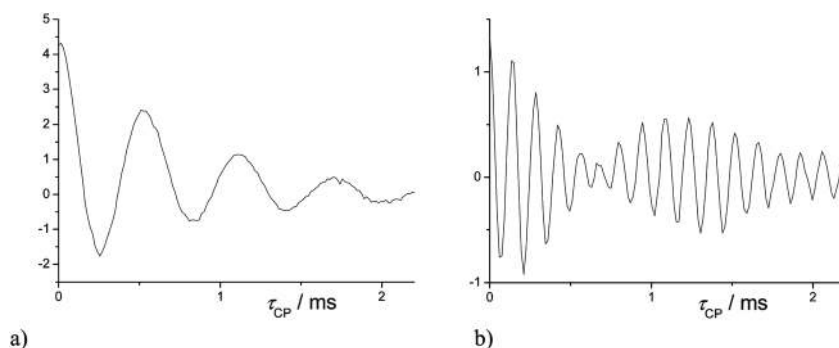


Fig. 13 ^{13}C interferograms representing the oscillatory polarization transfer between ^1H and ^{13}C for **4i**, carbon positions C9 and C11 (a) and C1 (b) (for numbering see Fig. 2).

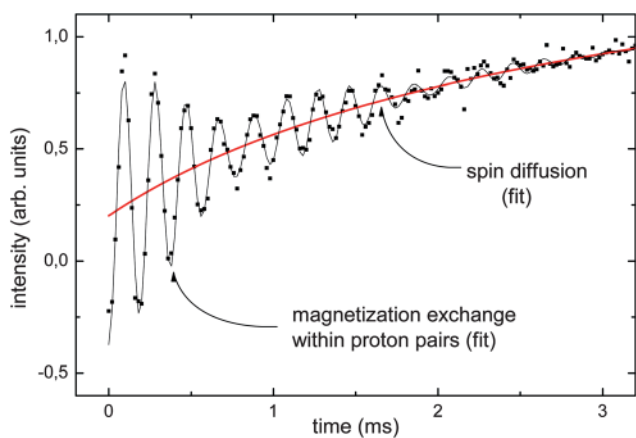


Fig. 14 Interferograms and spectra representing the oscillatory polarization transfer between neighbored protons; for example: **4i**, the protons attached to C1 had inverted polarization at $t_d = 0$; we observe the oscillatory polarization exchange with the protons attached to C2 and C2i (for numbering see Fig. 2).

out to be 138° (**4i**) and 144° (**5j**). In the case of fast fluctuating conformations these values are to be regarded as time averages over the angles belonging to the different conformations.

The conformation of the alkyl chains might be of some interest. Although the unknown order parameter of the hydrocarbon chain prevents an analysis of the tilt it seems to be very likely that the chains are oriented in average parallel to the magnetic field, *i.e.* to the molecular long axis. This might be concluded from the remarkable strong couplings, decreasing towards the chain end. Assuming tilts which are essentially different from zero would lead to unrealistic values of the order parameter.

3.8 Quantum chemical studies on the conformational behaviour of three-ring bent core mesogens

Conformational studies on three-ring bent-core molecules of the 1,3-phenylene type were performed using the density functional method (DFT) on the B3LYP/6-31G(d) level within the program package Gaussian 03.⁵⁴ The applicability of the method for the calculation of structural and electronic properties of larger molecules was indicated.⁵⁵ The energetically preferred structures

were obtained by full optimisation from different starting conformations.

Experimental investigations discussed before have shown that both the direction of the ester linkage groups and a lateral attached methyl group significantly change the mesogenic behaviour of the compounds (see Table 1).

Therefore, we have carried out conformational calculations on the isolated molecules having the aromatic core structures of compounds **1a**, **2a**, **1b** and **2b** (Table 1) to study the effect of the structural modifications mentioned before in these species. In order to reduce the computational effort we have generally used hexyloxy wing-groups for the considered molecules.

The conformational flexibility, dipole moments and bending angles were considered with respect to the orientation of the outer phenyl rings.

First, we have calculated the relaxed conformational barriers related to the torsion angle ϕ_1 resulting from a rotation of the carboxylic group with the central ring, that is around the C–O bond on the resorcinol derivatives **1a** and **2a** (rotation around C3 of the central phenyl ring and the O-atom of the ester group) and the C–C bond on the iso-phthalic acid esters **1b** and **2b** (rotation around C3–C6, for numbering see Fig. 2). The one-fold potential energy surface scans were generated by fixing of the corresponding torsion angle and complete optimisation of the other parameters in a stepwise manner. The results are illustrated in

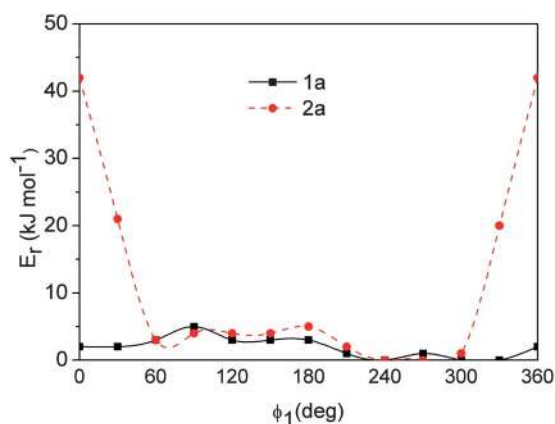


Fig. 15 Relaxed rotational barriers related to the torsion angle $\phi_1/\text{C-O}$ for the systems **1a** and **2a**.

Fig. 15 and 16 for these molecules. It is remarkable that the influence of a lateral methyl group attached to position 2 strongly depends on the orientation of the ester linkage groups.

In the resorcinol esters (**1a**, **2a**) the substitution by a lateral methyl group causes a significant increase of the rotational barrier. The flexibility of the segments, especially the free rotation about the C–O bond, is limited in **2a** (Fig. 15). The isophthalic esters show a different conformational behaviour with respect to the methylation in the 2-position. The 2-methyl-isophthalic ester (**2b**) has a significantly lower rotational barrier related to the C–C bond with the central ring in comparison to the iso-phthalic ester (**1b**). Obviously, the methylation of **1b** causes especially in the energetically preferred areas of **1b** ($\phi_1 = 0^\circ, 180^\circ$) a larger sterical stress which leads to a higher total energy and overall to a lower barrier of **2b**. Subject to the orientation of the ester connecting groups an attached methyl group in position 2 determines the conformational flexibility in the three-ring bent-core molecules in a different way.

Second, the bending angles α_1 of the molecules were calculated with respect to the torsion angle ϕ_1 of the C–O bond (**1a**, **2a**) and C–C bond (**1b**, **2b**) with the central ring. The bending angle for the three-ring ester with a central 1,3-phenylene unit was defined by a simple model from the central points of the three rings already used in an earlier paper.⁵⁵

The results are summarized in Fig. S2†. A comparison of the resorcinol ester (**1a**, **2a**) indicates that the α_1 values are about 120° over the whole area of the scan without any effect of the lateral methyl group. On the other hand in the iso-phthalic ester (**1b**, **2b**) the bending angle α_1 shows a significant dependence on the orientation of the rings. The α_1 values are in the range between 90° and 130° . It is remarkable that the methylation causes an increase of the bending angle in **2b**, especially in the energetically preferred conformers ($\phi_1 = 0^\circ, 30^\circ$) up to 130° . Moreover, in the most stable conformation of **2b** ($\phi_1 = 22^\circ$) generated by full optimisation a bending angle of 155° was obtained. In the energetically preferred conformation of **1b** ($\phi_1 = 180^\circ$) the α_1 value is about 90° , only. The significant effect is illustrated by an alignment of the most stable conformers of **1b** and **2b** with respect to three atoms of the central ring (Fig. 17). The results are in agreement with X-ray investigations on compound **2b** which indicated a bending angle of 156° for the molecules in the solid state, see Section 3.3.

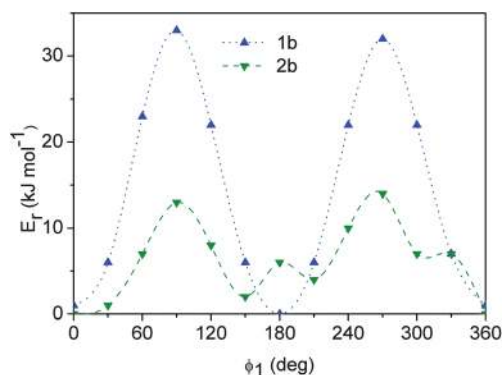


Fig. 16 Relaxed rotational barriers related to the torsion angle ϕ_1 /C–C for the systems **1b** and **2b**.

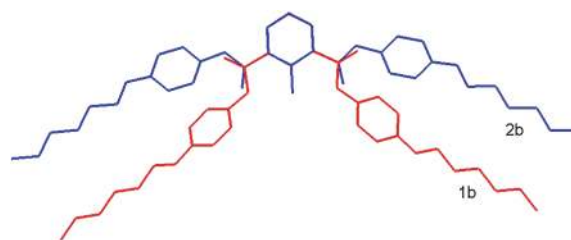


Fig. 17 Alignment of the most stable conformers of the iso-phthalic esters **1b** and **2b**, rotation around the C3–C6 bond (for numbering see Fig. 2) Red line: isophthalic ester **1b**, blue line: 2-methyl-isophthalic ester **2b**.

Third, the dependence of the dipole moments μ on the orientation of the rings in the bent-core molecules is illustrated in Fig. S3†. The attached methyl group has no significant effect on the dipole moments in both ester types.

Obviously, the larger differences between the μ values of the iso-phthalic acid and resorcinol esters result from the different orientation of the ester connecting groups.

The significant conformational effects of the methyl group in the isolated molecule **2b** may be seen in some way as a hint for the generation of the mesogenic properties of this compound.

The computations were performed on the SMP cluster of the computational centre of the Martin Luther University Halle-Wittenberg.

4. Conclusion

Usually, terminally substituted molecules consisting of three phenyl rings in which both outer rings are attached at the 1,3-positions of the central phenyl ring do not form liquid crystalline phases, provided that special effects caused by micro-segregation and hydrogen bonds are excluded. In the present paper three-ring bent-core bis(4-subst.-phenyl) 2-methyl-isophthalates are reported. Their liquid crystalline behaviour seems to be in contrast to the generally accepted relationships between the molecular structure and mesophase behaviour. For this reason, the goal of the paper was not only the characterization of the mesophases and their physical properties but also to find out why only this type of molecules (looking at Table 1) forms liquid crystalline phases. We employed an arsenal of methods (polarizing optical microscopy, calorimetry, X-ray diffraction in the solid and liquid crystalline states, solid state NMR spectroscopy, quantum chemical calculations, electrooptical, dielectric measurements, and SHG studies) to understand these questions.

The polarizing optical microscopy and calorimetric studies prove the existence of nematic, SmA and SmC phases that in first glance is similar to that of corresponding calamitic materials.

X-Ray crystal structure analysis proved that the bending angle is not near to 120° as expected for diphenyl isophthalate and reported for 2-methylresorcinol dibenzoates, but it is extended to 156° . Quantum chemical studies on the conformation of single three-ring bent-core molecules also show that the bending angle is about 155° . This increase of the opening angle (and therefore the decrease of the bending) is caused by the lateral methyl group in position 2 of the central phenyl ring.

Furthermore, solid state NMR investigations in the liquid crystalline phases prove that the angle between the two legs of the three-ring compounds turns out to be 138° in the SmA phase (**4i**) and 144° in the nematic one (**5j**). That means the molecules are more bent in the liquid crystalline states than in the crystalline one.

The layer spacing determined by X-ray diffraction studies of the SmA and SmC phases is either consistent with an overall bent-shape, or with strong intercalation between nearly rod-like molecules. In the nematic phase smectic clusters similar to those in usual five-ring bent-core nematics were found.

It follows from dielectric and SHG measurements that the SmA phase possesses a polar structure in an electric field. Furthermore, by the application of sufficiently high electric fields the SmA phase shows not only a slight change of the optical texture but also a clear polar current response from which an induced polarization of about 200 nC cm^{-2} could be determined. This behaviour may be attributed to the existence of randomly oriented polar clusters which obviously also remain in the isotropic phase sufficiently close to the clearing point.

Dielectric measurements of compound **4i** give a relaxation frequency for the reorientation about the molecular long axis much lower as observed for SmA phases formed by rod-like molecules. This can be interpreted as a tendency to form polar clusters, too.

Surprisingly, also in the isotropic liquid an induced polarization could be measured. But, in contrast to the SmA phase, this polarization was found to be proportional to the cell thickness. Therefore we can assume that this polarization mainly results from the accumulation of ionic charges on the electrodes. This process is connected with a clear increase of conductivity on the transition from the SmA to the isotropic liquid phase. Obviously, the ionic contribution is to a large extent absent in the smectic phase probably due to the larger relaxation time of the ionic contribution and the smaller conductivity in the SmA phase.

The existence of clusters in the isotropic phase of some bent-core mesogens has been proved by NMR spectroscopy.⁴⁶ Even in the smectic and isotropic phase, such clusters were recently found in binary mixtures of some bent-core and rod-shaped molecules.⁴⁷ The field induced orientation of the clusters also accounts for the slow dynamics. The reduction of the switching time with increasing temperature can be attributed to a decrease of the cluster size and of the viscosity of the continuous medium. The increase of the current at increasing temperature under constant electric fields is probably due to the increasing slope of the Langevin process at higher temperatures. We note that a similar electric current behaviour was also found in the nematic and isotropic phase of **5j**, where the smectic clusters were clearly seen in SAXS measurements.

To summarize, the liquid crystalline behaviour of three-ring bent-core bis(4-subst.-phenyl) 2-methyl-iso-phthalates can be understood by the extended bending angle caused by the lateral methyl group. The properties of the mesophases are different from those formed by calamitic mesogens and also from those of four-ring or five-ring bent-core compounds. Unusual behaviour and interesting properties can be expected for such materials existing at the boundary between calamitic liquid crystals and banana-shaped liquid crystals.

For additional information on experimental procedures, analytical data, X-ray data, and quantum chemical calculations, see ESI†.

Acknowledgements

AJ acknowledges financial support from NSF DMR-0964765 and useful discussions with Drs Spunt and J. Gleeson. AE thanks H. Takezoe for the opportunity to use equipment for electro-optical and dielectric measurements.

References

- 1 D. Vorländer, Die Erforschung der molekularen Gestalt mit Hilfe kristallinischer Flüssigkeiten, *Z. phys. Chem.*, 1923, **105**, 211–254.
- 2 G. Pelzl, S. Diele and W. Weissflog, *Adv. Mater.*, 1999, **11**, 707–724.
- 3 R. Amarantatha Reddy and C. Tschierske, *J. Mater. Chem.*, 2006, **16**, 907–961.
- 4 H. Takezoe and Y. Takanishi, *Jpn. J. Appl. Phys.*, 2006, **45**, 597–625.
- 5 W. Weissflog, U. Dunemann, S. Findeisen-Tandel, M.-G. Tamba, H. Kresse, G. Pelzl, S. Diele, U. Baumeister, A. Eremin, S. Stern and R. Stannarius, *Soft Matter*, 2009, **5**, 1840–1847, and references given therein.
- 6 R. Deb, R. K. Nath, M. K. Paul, N. V. S. Rao, F. Tuluri, Y. Shen, R. Shao, D. Chen, C. Zhu, I. I. Smalyukh and N. A. Clark, *J. Mater. Chem.*, 2010, **20**, 7332–7336.
- 7 M. B. Chauhan, D. K. Bhoi, M. T. Machhar, D. K. Solanki and D. Solanki, *Der Pharma Chemica*, 2010, **2**(4), 30–37.
- 8 B. Das, S. Grande, W. Weissflog, A. Eremin, M. W. Schröder, G. Pelzl, S. Diele and H. Kresse, *Liq. Cryst.*, 2003, **30**, 529–539.
- 9 F. C. Yu and L. J. Yu, *Chem. Mater.*, 2006, **18**, 5410–5420.
- 10 E. Enz, S. Findeisen-Tandel, R. Dabrowski, F. Giesselmann, W. Weissflog, U. Baumeister and J. Lagerwall, *J. Mater. Chem.*, 2009, **19**, 2950–2957.
- 11 K. Kishikawa, S. Furusawa, T. Yamaki, S. Kohmoto, M. Yamamoto and K. Yamaguchi, *J. Am. Chem. Soc.*, 2002, **124**, 1597–1605.
- 12 R. Judele, S. Laschat, A. Baro and M. Nimtz, *Tetrahedron*, 2006, **62**, 9681–9687.
- 13 K. Kishikawa, K. Oda, S. Aikyo and S. Kohmoto, *Angew. Chem., Int. Ed.*, 2007, **46**, 764–768.
- 14 H. Shimura, M. Yoshio, A. Hamasaki, T. Mukai, H. Ohno and T. Kato, *Adv. Mater.*, 2009, **21**, 1591–1594.
- 15 C. Su, L. X. Lee, S. H. Yu, Y. K. Shih, J. C. Su, F. J. Li and C. K. Lai, *Liq. Cryst.*, 2004, **31**, 745–749.
- 16 D. M. Huck, H. L. Nguyen, B. Donnio and D. W. Bruce, *Liq. Cryst.*, 2004, **31**, 503–507.
- 17 K. Kishikawa, S. Nakahara, Y. Nishikawa, S. Kohmoto and M. Yamamoto, *J. Am. Chem. Soc.*, 2005, **127**, 2565–2571.
- 18 J. Malthe, A. M. Levelut and L. Liebert, *Adv. Mater.*, 1992, **4**, 37–41.
- 19 L. Kovalenko and W. Weissflog, will be published elsewhere.
- 20 L. Zou, J. Wang, V. J. Beleva, E. E. Kooijman, S. V. Primak, J. Risse, W. Weissflog, A. Jakli and E. K. Mann, *Langmuir*, 2004, **20**, 2772–2780.
- 21 S. I. Torgova, T. A. Geivandova, O. Francescangeli and A. Strigazzi, *Pramana*, 2003, **61**, 239–248.
- 22 S. Kang, Y. Saito, N. Watanabe, M. Tokita, Y. Takanishi, H. Takezoe and J. Watanabe, *J. Phys. Chem. B*, 2006, **110**, 5205–5214.
- 23 H. Galardo, A. J. Bortoluzzi and D. M. P. de O. Santos, *Liq. Cryst.*, 2008, **35**, 719–725.
- 24 J. H. Wild, K. Bartle, N. T. Kirkman, S. M. Kelly, M. O’Neill, T. Stirner and R. P. Tuffin, *Chem. Mater.*, 2005, **17**, 6354–6360.
- 25 J. Han, X. Y. Chang, L. R. Zhu, Y. M. Wang, J. B. Meng, S. W. Lai and S. Y. Chui, *Liq. Cryst.*, 2008, **35**, 1379–1394.
- 26 C. H. Lee and T. Yamamoto, *Mol. Cryst. Liq. Cryst. Sci. Technol., Sect. A*, 2001, **369**, 95–102.
- 27 Y. Tang, Y. Wang, X. Wang, S. Xun, C. Mei, L. Wang and D. Yan, *J. Phys. Chem. B*, 2005, **109**, 8813–8819.
- 28 P. V. Chalapathi, M. Shrinivasulu, B. V. S. Goud, G. K. M. Pisipati and D. M. Potukuchi, *Ferroelectrics*, 2005, **322**, 53–67; P. V. Chalapathi, M. Srinivasulu, G. K. M. Pisipati,

- C. H. Satyanarayana and D. M. Potukuchi, *Phys. B*, 2011, **406**, 2081–2090.
- 29 V. C. Pallavajhula, M. Shrinivasulu, G. K. M. Pisipati and D. M. Potukuchi, *Ferroelectrics*, 2007, **361**, 45–61.
- 30 Y. M. Huang and Q.-L. Ma, *Liq. Cryst.*, 2010, **37**, 1119–1126.
- 31 W. Weissflog, *Liq. Cryst.*, 2011, **38**, 1081–1083.
- 32 K. A. Hope-Ross, P. A. Heiney and J. F. Kadla, *Can. J. Chem.*, 2010, **88**, 639–645.
- 33 W. Maier and K. Markau, *Z. phys. Chem. (Neue Folge)*, 1961, **28**, 190–202.
- 34 V. F. Petrov, E. P. Pozidaev, A. L. Andreev, I. N. Kompanets and Y. Shimizu, *Mol. Cryst. Liq. Cryst. Sci. Technol., Sect. A*, 2001, **363**, 97–106.
- 35 T. Tasaka, H. Okamoto, V. F. Petrov and S. Takkenaka, *Liq. Cryst.*, 2001, **28**, 1025–1034.
- 36 T. Tasaka, H. Okamoto, Y. Morita, K. Kasatani and S. Takenaka, *Liq. Cryst.*, 2003, **30**, 961–977.
- 37 R. Vadnais, M. A. Beaudoin, A. Beaudoin, B. Heinrich and A. Soldera, *Liq. Cryst.*, 2008, **35**, 357–364.
- 38 W. Weissflog, G. Naumann, B. Kosata, M. W. Schroeder, A. Eremin, S. Diele, H. Kresse, R. Friedemann and S. Ananda Rama Krishnan, *J. Mater. Chem.*, 2005, **15**, 4328–4337.
- 39 R. A. Reddy, U. Baumeister, J. L. Chao, H. Kresse and C. Tschierske, *Soft Matter*, 2010, **6**, 3883–3897.
- 40 S. Diele, S. Grande, H. Kruth, Ch. Lischka, G. Pelzl, W. Weissflog and I. Wirth, *Ferroelectrics*, 1998, **212**, 169–177.
- 41 J. M. Adams and S. E. Morsi, *Acta Crystallogr., Sect. B: Struct. Crystallogr. Cryst. Chem.*, 1976, **32**, 1345–1347.
- 42 P. Birner, S. Kugler, K. Simon and G. Naray-Szabo, *Mol. Cryst. Liq. Cryst.*, 1982, **80**, 11–17.
- 43 U. Baumeister, W. Brandt, H. Hartung and M. Jaskolski, *J. Prakt. Chem.*, 1983, **325**, 742–752.
- 44 Ch. Keith, M. Prehm, Y. P. Panarin, J. K. Vij and C. Tschierske, *Chem. Commun.*, 2010, **46**, 3702–3704.
- 45 K. Miyasato, S. Abe, H. Takezoe, A. Fukuda and E. Kuze, *Jpn. J. Appl. Phys.*, 1983, **22**, L661–L663.
- 46 V. Dominici, *Soft Matter*, 2011, **7**, 1589–1598.
- 47 S. H. Hong, R. Verduzco, J. T. Gleeson, S. Sprunt and A. Jakli, *Phys. Rev. E: Stat., Nonlinear, Soft Matter Phys.*, 2011, **83**, 061702.
- 48 A. Eremin, H. Nadasi, G. Pelzl, H. Kresse, W. Weissflog and S. Grande, *Phys. Chem. Chem. Phys.*, 2004, **6**, 1290–1298.
- 49 G. Pelzl, S. Diele, S. Grande, A. Jakli, C. Lischka, H. Kresse, H. Schmalfuss, I. Wirth and W. Weissflog, *Liq. Cryst.*, 1999, **26**, 401–413.
- 50 J. Xu, K. Fodor-Csorba and R. Y. Dong, *J. Phys. Chem. A*, 2005, **109**, 1998–2005.
- 51 M. Lee and W. I. Goldberg, *Phys. Rev. A: At., Mol., Opt. Phys.*, 1965, **140A**, 1261–1271.
- 52 B. J. van Rossum, C. P. de Groot, V. Ladizhansky, S. Vega and H. J. M. de Groot, *J. Am. Chem. Soc.*, 2000, **122**, 3465–3472.
- 53 M. Roos, P. Micke and G. Hempel, *Chem. Phys. Lett.*, submitted.
- 54 M. J. Frisch, G. W. Trucks, H. B. Schlegel, G. E. Scuseria, M. A. Robb, J. R. Cheeseman, J. A. Montgomery, Jr, T. Vreven, K. N. Kudin, J. C. Burant, J. M. Millam, S. S. Iyengar, J. Tomasi, V. Barone, B. Mennucci, M. Cossi, G. Scalmani, N. Rega, G. A. Petersson, H. Nakatsuji, M. Hada, M. Ehara, K. Toyota, R. Fukuda, J. Hasegawa, M. Ishida, T. Nakajima, Y. Honda, O. Kitao, H. Nakai, M. Klene, X. Li, J. E. Knox, H. P. Hratchian, J. B. Cross, V. Bakken, C. Adamo, J. Jaramillo, R. Gomperts, R. E. Stratmann, O. Yazyev, A. J. Austin, R. Cammi, C. Pomelli, J. W. Ochterski, P. Y. Ayala, K. Morokuma, G. A. Voth, P. Salvador, J. J. Dannenberg, V. G. Zakrzewski, S. Dapprich, A. D. Daniels, M. C. Strain, O. Farkas, D. K. Malick, A. D. Rabuck, K. Raghavachari, J. B. Foresman, J. V. Ortiz, Q. Cui, A. G. Baboul, S. Clifford, J. Cioslowski, B. B. Stefanov, G. Liu, A. Liashenko, P. Piskorz, I. Komaromi, R. L. Martin, D. J. Fox, T. Keith, M. A. Al-Laham, C. Y. Peng, A. Nanayakkara, M. Challacombe, P. M. W. Gill, B. Johnson, W. Chen, M. W. Wong, C. Gonzalez and J. A. Pople, *Gaussian 03, Revision D.1*, Gaussian, Inc, Wallingford CT, 2005.
- 55 S. Ananda Rama Krishnan, W. Weissflog, G. Pelzl, S. Diele, H. Kresse, Z. Vakhovskaya and R. Friedemann, *Phys. Chem. Chem. Phys.*, 2006, **8**, 1170–1177.